

Żur, et al., 2022

Volume 8, pp. 01-16

Received: 30th September 2021

Revised: 10th February 2022, 17th February 2022

Accepted: 19th February 2022

Date of Publication: 15th March 2022

DOI- <https://doi.org/10.20319/mijst.2022.8.0116>

This paper can be cited as: Żur, A., Zur, P. & Bajer, A. (2022). *Fem Analysis of Wooden Joints and Wooden Structure of the Electric Car's Frame*. *MATTER: International Journal of Science and Technology*, 8, 01-16.

This work is licensed under the Creative Commons Attribution-NonCommercial 4.0 International License. To view a copy of this license, visit <http://creativecommons.org/licenses/by-nc/4.0/> or send a letter to Creative Commons, PO Box 1866, Mountain View, CA 94042, USA

FEM ANALYSIS OF WOODEN JOINTS AND WOODEN STRUCTURE OF THE ELECTRIC CAR'S FRAME

Alicja Żur

Department of Engineering Processes Automation, Integrated Manufacturing Systems, Faculty of Mechanical Engineering, Silesian University of Technology, Gliwice, Poland
alicja.zur@polsl.pl

Pawel Żur

Department of Engineering Processes Automation, Integrated Manufacturing Systems, Faculty of Mechanical Engineering, Silesian University of Technology, Gliwice, Poland
pawel.zur@polsl.pl

Andrzej Baier

Prof. PŚ, Department of Engineering Processes Automation, Integrated Manufacturing Systems, Faculty of Mechanical Engineering, Silesian University of Technology, Gliwice, Poland
andrzej.baier@polsl.pl

Abstract

The paper covers the topic of FEM analysis (Finite Element Method) of selected types of wood joints and the analysis of the wooden structure, the electric car in the electric car of the frame of the Silesian Greenpower team. The main assumption of the work was to analyze the displacements

and stresses in the structure of the frame that result from the actual load on the structure. Selected wooden joints were analyzed in FEM analysis. The paper also presents various techniques for modelling connections between elements, such as connection by nail or screw, cohesive contact, or the MPC beam element considering three different materials: oak, pine, and plywood. The aim of the study and the final stage was the FEM analysis of the wooden structure, the car frame. The actual support points for the frame and the actual loads on the structure resulting from the mass of components such as the driver, batteries, and motor were taken into account. The distribution and values of stresses in the structure were analysed, as well as the total displacements resulting from the loading of the mass elements, as well as the centrifugal force acting on the car during driving in a corner.

Keywords

Electric Vehicle, FEM Analysis, Glue Joint, Screw Joint, Wood Joints, Wood Structure

1. Introduction

This paper deals with the FEM analysis (Finite Element Method) of joints of wooden structures. The aim of the project was the FEM analysis of selected types of carpentry joints and the analysis of a wooden structure - the frame of the Silesian Greenpower team car. Wooden joints were chosen because of the advantages such as simplicity of manufacture, wide availability of material and lack of highly specialized tooling or qualifications needed to perform the joint. FEA analysis was chosen because of its wide applicability and the wide availability of software to perform this type of mechanical and strength analysis software.

2. Literature Review

Wood as a construction material has been known to men for many centuries. Its wide availability and the possibility of machining and forming have already been appreciated in ancient times. The first wooden structures, wooden huts, in northern Europe date back to the Bronze Age, around 3500 BC. For centuries, wood has been used to create buildings, as well as structures and utility items such as ships, boats, and furniture. In ancient Rome, measuring tools such as wooden calipers were made. Over the centuries, woodworking and carpentry played an important role in architecture, religion, and agriculture (Apay, 2012; Baier, Grabowski, Stebel, Komander, Konopka, Kołodziej & Żur, 2018; Bąk & Burczyński, 2001).

To this day, the reasons why wood is selected as a building material are its properties, such as durability, ease of construction, or heat insulation, which in some climatic conditions is still the most important factor (Groom, Mott & Shaler, 2002).

Today, wooden structures, especially in construction and furniture, are being revived due to trends such as ecology, the care of the environment, and the desire to be closer to nature (Bak & Burczyński, 2001). The mechanical characteristics and strength of wood as an anisotropic material consist of many components. Static properties are determined in samples with fibres arranged along and across the fibres. Among the determined properties, the following can be mentioned: tensile strength, compressive strength, shear strength, bending strength, modulus of elasticity (for the same loads). The technological properties of wood, such as hardness and cleavage, are also determined (Groom, Mott & Shaler, 2002).

The finite element method, or FEM for short, has played a special role in testing the strength of materials for more than 40 years. It is a numerical method that, together with the proliferation of computers, caused a real revolution in the field of strength calculations (Hunt, 2004; Jasiński, Nowak & Karolak, 2014).

The finite element method (FEM) is the dominant technique of strength analysis in structural mechanics. The basic concept in the physical interpretation of FEM is the division of the mathematical model into disjoint (non-overlapping) components of simple geometry called "finite elements," or elements for short. The reaction of each element is expressed as a finite number of degrees of freedom characterized as the value of an unknown function or function in the set of nodal points. The response of the mathematical model is considered to be approximative to the response of the discrete model obtained by combining or assembling a set of all elements (Hunt, 2004; Jasiński, Nowak & Karolak, 2014; Karaöali & Ulguel, 2014; Štědroňová, 2010; Tankut, Tankut & Zor, 2014).

3. Research Issue

The purpose of this study was to perform a numerical FEM analysis for the electric race car in the electric racing car of the frame of the Silesian Greenpower team electric racing car. First, a preliminary FEA analysis of the different types of wood joints (here a nail joint and a glued joint) should be carried out taking into account the different materials. The orthotropic material properties of wood must also be taken into account.

4. Materials and Methods

The present study consisted of two stages - first, FEM analysis of selected timber joints was performed in ANSYS Mechanical 19.2. Academic software. The FEM analysis methodology is presented below. The analysis considered the orthotropic material properties of two different types of wood, oak and pine. The analysis was also performed for wood plywood to compare the results of orthotropic materials with isotropic materials. The results from the FEM analysis of the individual joints were then used for the FEM analysis of the entire frame. The following section describes the process of preparing the CAD model for analysis as well as the analysis itself.

4.1. FEM Analysis of Wooden Joints

The first stage of the research was the FEM analysis of individual wooden joints. For this purpose, the following connections were selected: screw joint and glued joint. The geometry for each model was prepared in Siemens NX. FEM analyzes were performed in ANSYS Workbench using the Mechanical module - Static Structural study type.

Three materials were analyzed for each joint, oak, pine, and plywood. Oak and pine wood have been modelled as orthotropic materials due to the different properties of the wood along and across the grain. Plywood has been modeled as an isotropic material that has the same properties in all directions. The properties of all three wood materials are presented in Table 1.

Table 1: *Orthotropic properties of oak and pine wood and isotropic properties of plywood*

		Oak	Pine	Plywood
Density [kg/m³]		0,6	0,5	0,917
Young's modulus [MPa]	Along the Fibres	10300	11200	5610
	Across the Fibres	1586	985	
Poissons ratio	X	0,35	0,347	0,245
	Y	0,448	0,315	
	Z	0,56	0,408	
	Along the Fibres	12400	12400	2253

Shear modulus [MPa]	Across the Fibres	8900	9500	
Tensile strength [MPa]	Along the Fibres	5,5	3,2	6,2
	Across the Fibres	5,1	1,93	

(source: Groom, Mott & Shaler, 2002; Hunt, 2004)

The first step was to analyze the screw joint. In this case, only half of the geometry was modeled and the plane of symmetry was included in the analysis parameters. Two types of contacts were used to connect the two boards to each other - frictional contact between the contact surfaces of the boards with a kinetic friction coefficient of 0.2 and the MPC element of the Beam Connection type in order to resemble the geometry and the connection between the surfaces of the nail hole. The behavior of the MPC element has been defined as perfectly rigid. Among the parameters of the MPC element, the so-called Pinball Region has been defined - the area representing the screw head that also interacts with the adjacent surface. The material assigned for this element is structural steel from the ANSYS library. The set diameter of the MPC element was 0.2 mm larger than the diameter of the hole (Tankut, Tankut & Zor, 2014). The mesh of the model has been presented in Fig. 1.

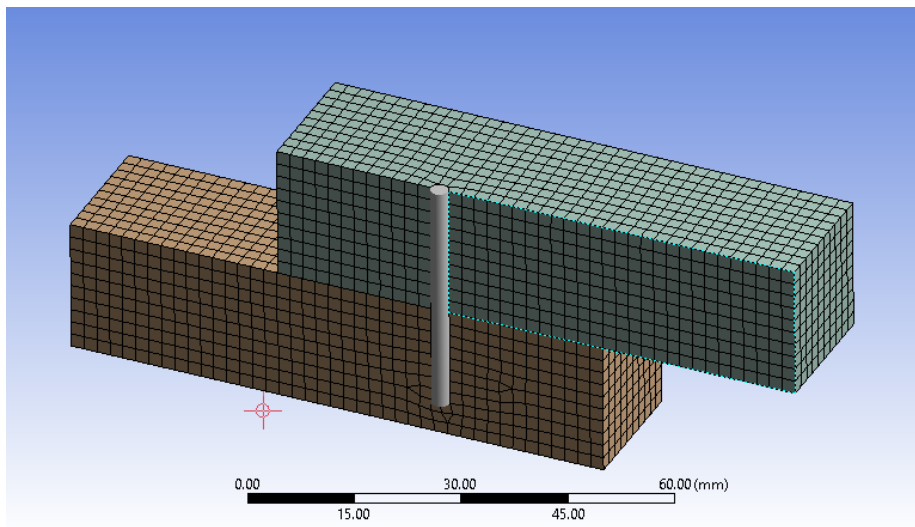


Figure 1: *Elements Connection using Beam Connection and an MPC Elements*
(source: own data)

A glued joint has characteristics different from those of a frictional (contact) joint or a screw joint. There is no weakening of the material by breaking its homogeneity as in the case of a joint with nails or screws. The properties of the joint itself, not only of the glued material, play an important role.

There are several methods for modelling adhesive joints. One of them is the actual modeling of a thin layer with given material properties; however, due to the size of the elements, this method is computationally time consuming. The second method used in this FEM analysis is to model the joint as a cohesive zone (CZM - Cohesive Zone Modelling) (Štědroňová, 2010; Tankut, Tankut & Zor, 2014; Zachariah, 2006).

No separate layer of adhesive material was present in the model, and the connection of elements was ensured by adopting the interaction in the form of cohesive contact. To do this, a material model was created to represent the properties of the glue. The properties of the CZM material are shown in Fig. 2.

	A	B	C	D	E
1	Property	Value	Unit		
2	Fracture-Energies based Debonding				
3	Debonding Interface Mode	Mixed			
4	Tangential Slip Under Normal Compression	No			
5	Maximum Normal Contact Stress	1.7E+06	Pa		
6	Critical Fracture Energy for Normal Separation	280	J m ⁻²		
7	Maximum Equivalent Tangential Contact Stress	1E-30	Pa		
8	Critical Fracture Energy for Tangential Slip	1E-30	J m ⁻²		
9	Artificial Damping Coefficient	1E-08	s		

Figure 2: Properties of CZM Material

(source: own data)

The joint geometry was modelled as touching 2D surfaces. The connection geometry is shown in Fig. 3. The element size for the mesh was assumed to be 2 mm. The orthotropic material is oriented in such a way that it has the greatest strength in the tensile direction.

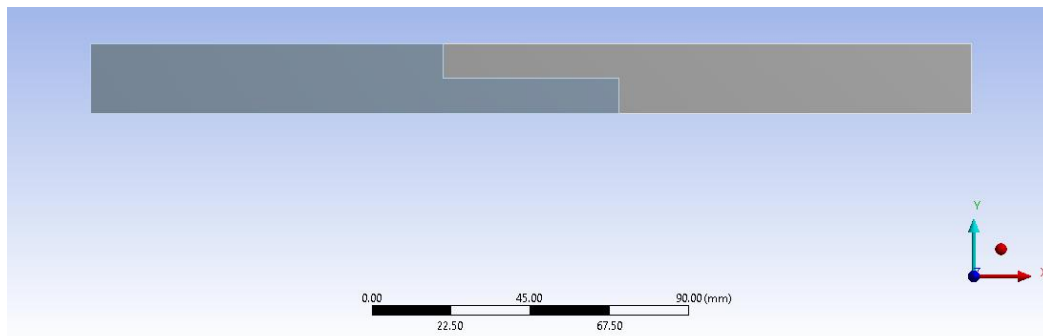


Figure 3: Geometry of the glue joint
(source: own data)

The next step was to establish contact between the elements. For this purpose, the type of bonded contact was adopted, and then the fracture contact debonding element was added, which is responsible for the cohesive connection of the tested joint. These parameters allow one to determine the force needed to break the connection. The joint was restrained at both ends and a force was applied perpendicular to the joint so that it would break. Due to the lack of occurrence of the glue layer in the model, the value and direction of the shear stresses were not determined. The purpose of using the model with cohesive contact justifies the possibility of verifying the distribution of normal stresses in the joined elements.

4.2. FEM Analysis of a Wooden Structure – Electric Bolide Frame

In this work, the FEM analysis of the wooden structure, the car frame of the Silesian Greenpower team, was also carried out. The structure of the car's frame should ensure stiffness while driving, even distribution of weight through the arrangement of batteries and motor and meet the safety requirements of the competition regulations. The safety elements are the front plate to which a foam with a specific compressibility is attached, which should suppress the frontal impact, the front rollbar above the driver's legs, and the rear rollbar, which are designed to protect the driver in the event of a possible fall and overturn of the vehicle (Baier, Grabowski, Stebel, Komander, Konopka, Kołodziej & Żur, 2018; Żur, Baier & Kołodziej, 2020).

The geometry of the car frame has been simplified to reduce computation time. The operations to which the frame model was subjected included replacement of the perforated front and rear plates with solid plates, removal of fillets at the battery box, and significant simplification of the geometry of the front and rear stub axle mounting. Half of the model was used for calculations and the symmetry condition was assumed. A simplified model prepared for FEM analysis is presented in Fig. 4.

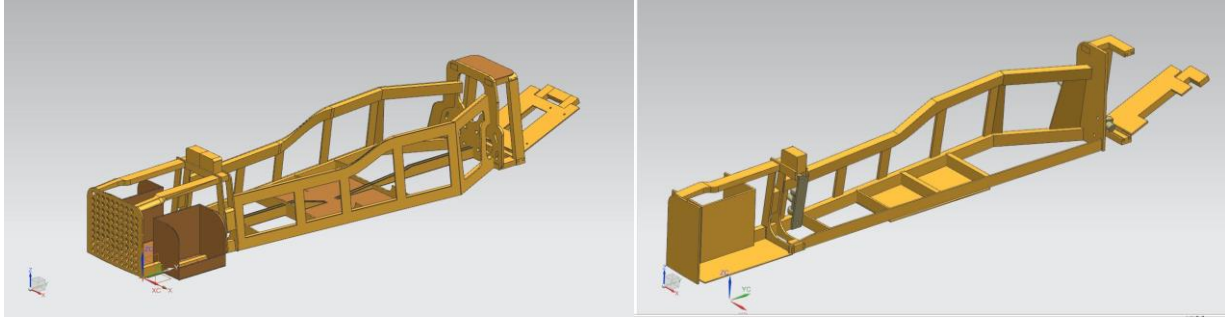


Figure 4: Geometry of the bolide's frame before simplifying (left) and after (right);
(source: own data)

Then, material properties were assigned to the imported geometry. The material used for the frame is plywood and for shafts Structural Steel from the ANSYS library.

The next step was to define the plane of symmetry. In this step, planes were added with the symmetry region option and intersection planes in the model were selected. The next step was to define the connections between the elements. The wooden elements were connected to each other with a bonding contact, while the steel subassemblies were connected to the wooden frame by means of the beam connection type, which reflects the bolted connections between the elements.

The next stage of the analysis was to determine the boundary conditions. The frame is fixed at the actual points of support, i.e. at the ends of the shafts. The forces adopted for the analysis are presented in Table 2. For all elements that load the structure, the force resulting from half of its mass was assumed because only half of the structure was tested. The boundary conditions of the analysis are presented in Fig. 5. A force corresponding to the weight of the driver is applied to the floor pan on which the driver's seat is attached. A force for the mass of the battery is applied to the lower surface of the battery box at the front of the frame, and a force for the mass of the motor is applied perpendicular to the motor mount plate at the rear of the frame.

Table 2: The loads applied to the structure adopted for the FEM analysis

Element	Weight [kg]	Force [N]
Driver	50	250
Batteries	24	120
Motor	5	25

(source: own data)

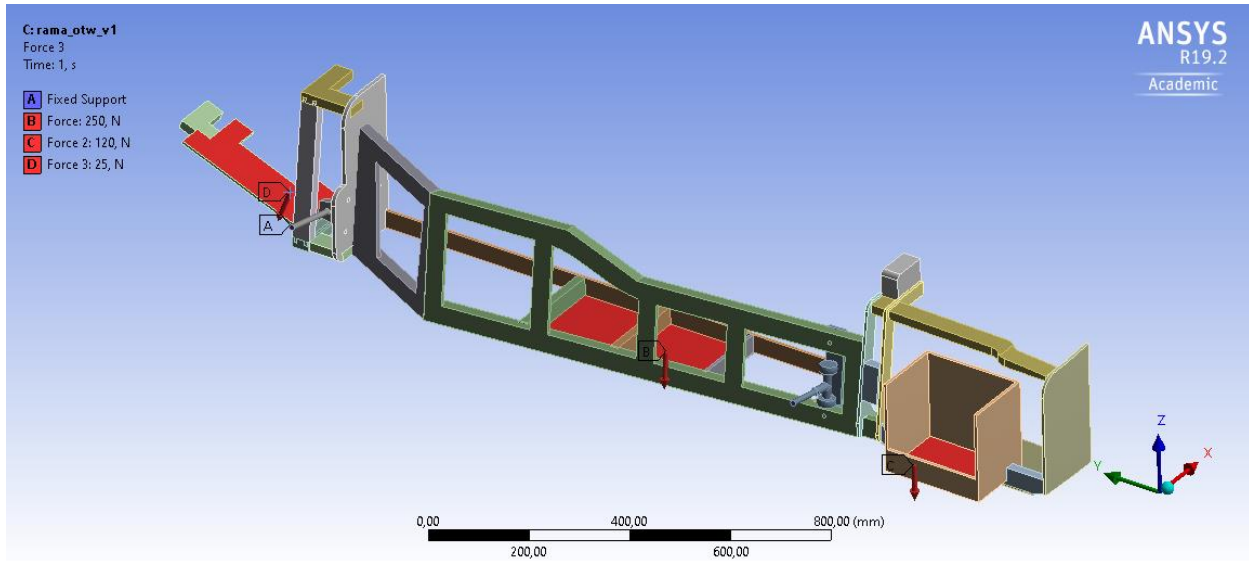


Figure 5: Boundary conditions of FEM analysis of structures

(source: own data)

In the last stage of the analysis, the stresses and displacements experienced by the frame structure during driving in a corner were examined - the influence of centrifugal force and aerodynamic drag force on the distribution of stresses and displacements in the frame structure was checked.

During the race, the speed achieved by the car is approximately 17 m / s. The corner chosen is the Luffield Corner at Silverstone, UK, where the league's annual final takes place. The radius of this turn is approximately 60 m. It is one of the most difficult corners a driver has to deal with on the tracks where a team starts.

Having the above information and knowing the weight of the car with the driver, that is about 103 kg, it is possible to calculate the centrifugal force acting on the car in a turn using the formula (1):

$$F_{cent} = \frac{m * v^2}{R}, \quad (1)$$

Where:

m - Weight of the car with the driver [kg],

v - Car speed [m / s],

R - Corner radius, [m].

The calculated centrifugal force was 496 N. The material parameters used in the analysis of the loads resulting from the mass of the objects remained unchanged. The mesh of the entire

frame model was made. A point has also been created that corresponds to the center of gravity of the entire car and the frame. At this point, the centrifugal force was applied. Then the point corresponding to the center of gravity was connected by MPC elements to the centers of gravity of the individual masses, the driver, batteries and motor (Fig. 6). The force resulting from the aerodynamic drag (approx. 9N) was evenly distributed at the points of attachment of the bodywork to the frame.

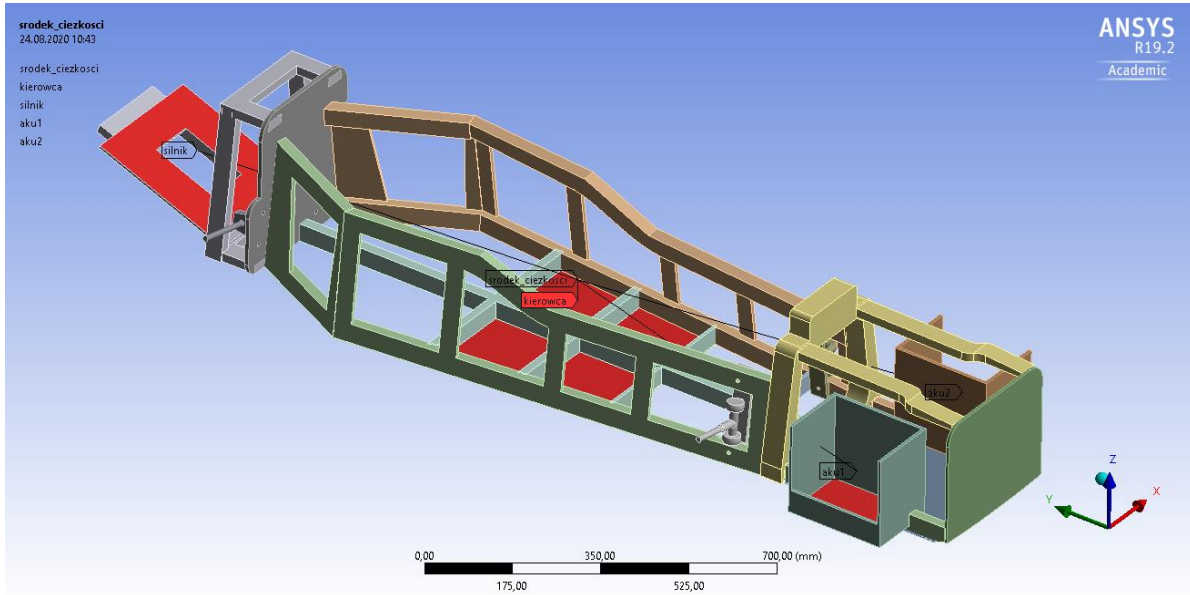


Figure 6: *Boundary conditions of the structure stress analysis in a corner*
(source: own data)

5. Results and Discussion

This section presents the results of the analyzes performed. First, the results of the FEM analysis for individual wood joints for a screw or nail and a glued joint. The results consider three different materials, oak wood, pinewood and plywood. Next, the results of the FEM analysis for the bolide frame are presented. The results were presented for static loads acting on the frame resulting from the masses of objects and simulated forces resulting from the vehicle driving in a curve.

5.1. FEM Analysis of Wooden Joints

FEM analysis of a screw or nail joint yielded von Mises-reduced stresses and displacements occurring in the joint under force application. In each tested material, the highest stresses occurred

at the same place (Fig. 7). These stresses are generated indirectly by the action of the screw head pressing the material of the board.

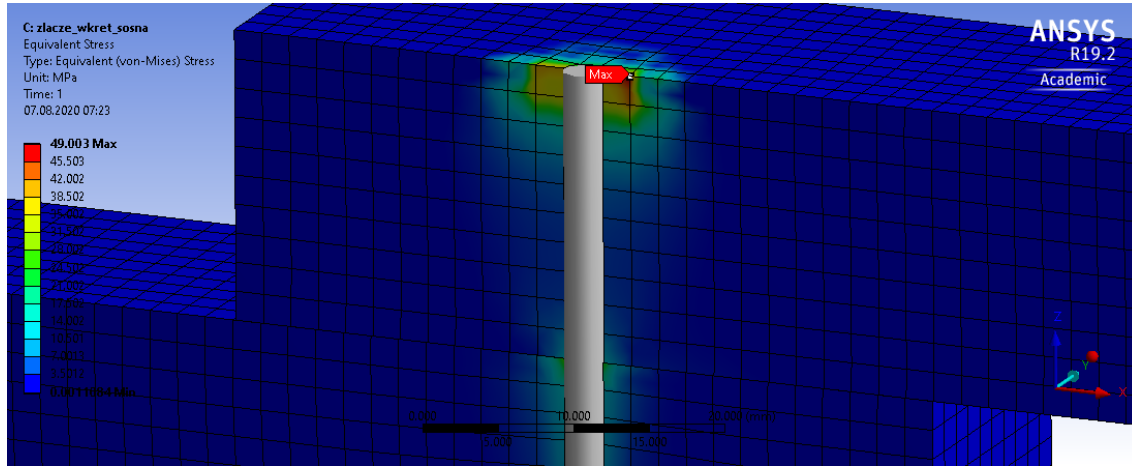


Figure 7: Place of occurrence of the greatest reduced stresses in all models
 (source: own data)

A summary of the results is presented in Table 3. The reduced stresses for oak wood obtained by FEM analysis were twice as high as for the other materials. They were 105.53 MPa compared to 49.03 MPa for pinewood and 54.29 MPa for plywood. The ratio of displacement results for oak wood is inversely proportional to the stresses. The displacements for oak (0.04054 mm) were twice those of pine wood (0.086451 mm) and three times those of plywood (0.12255 mm).

Table 3: The displacements and stresses obtained in the FEM analysis of the screw joint

	Oak	Pine	Plywood
Stress [MPa]	105,53	49,03	54,29
Displacement [mm]	0,04054	0,086451	0,12255

(source: own data)

FEA analysis of the adhesive joint also determined the von Mises-reduced stresses and displacements that occur in the joint under force application. The comparison of the results is presented in Table 4. The reduced stresses obtained from the FEA analysis are similar for each of the models used. The stresses for oak and pine wood are very similar, 17.622 MPa, and 17.624 MPa respectively, giving a difference of 0.1%. The reduced stress for the plywood was 17.453 MPa, which is a difference of less than 1% from the other results. The displacements obtained in

the analysis are different for each model. 0.49 mm for oak wood, 1.2 mm for pine wood (2.5 times more) and 2 mm for particleboard (4 times more with respect to oakwood)

Table 4: *The displacements and stresses obtained in the FEM analysis of the glue joint*

	Oak	Pine	Plywood
Stress [MPa]	17,622	17,624	17,453
Displacement [mm]	0,49289	1,2082	2,0017

(source: own data)

The stress distribution in a bonded joint using isotropic material is shown in Fig. 8.

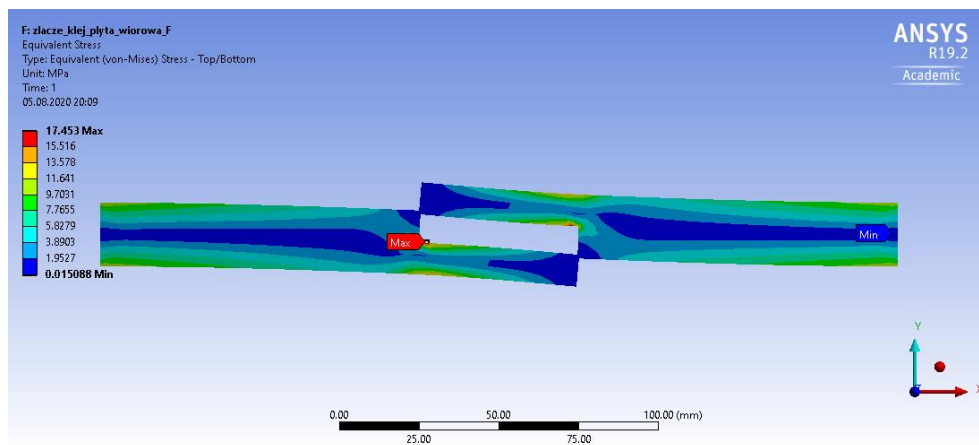


Figure 8: *Reduced stress distribution in a glued joint with isotropic wood material*

(source: own data)

5.2. FEM Analysis of a Wooden Structure – Electric Bolide Frame

As a result of the analysis, the total displacements in the structure and stresses (von Mises) were obtained. The maximum displacement was 2.95 mm and occurred in the area of the highest load, under the driver's seat. The displacement in the area of the battery mount was 1.6 mm, while in the area of the plate under the motor it was 2.4 mm.

The greatest stresses were observed in the place where the element was supported, at the ends of the shafts. The maximum stress was 87.4 MPa and occurred at the end of the front shaft. There are also areas where the axle interacts with the frame, the area around the bolts that attach the axle to the frame. There, the stresses amounted to approximately 5 MPa.

Increased stresses were also noted in the area of the driver's seat - there the stresses fluctuated up to 14 MPa. Despite the highest load, the stress distribution at this point is even.

The area of increased stresses was also the area of rear shaft mounting, at the support point, that is, at the shaft end, the stresses amounted to 16 MPa. The stresses resulting from the connection of the shaft to the frame amount to approximately 3-4 MPa, while the stresses in the plate under the motor are approximately 5 MPa. Increased stress, approx. 13 MPa, also occurs at the boundary of the first stage of the shaft, but due to the simplified geometry, there is only one shaft stage, so there is also a stress concentration at this point (Fig. 9).

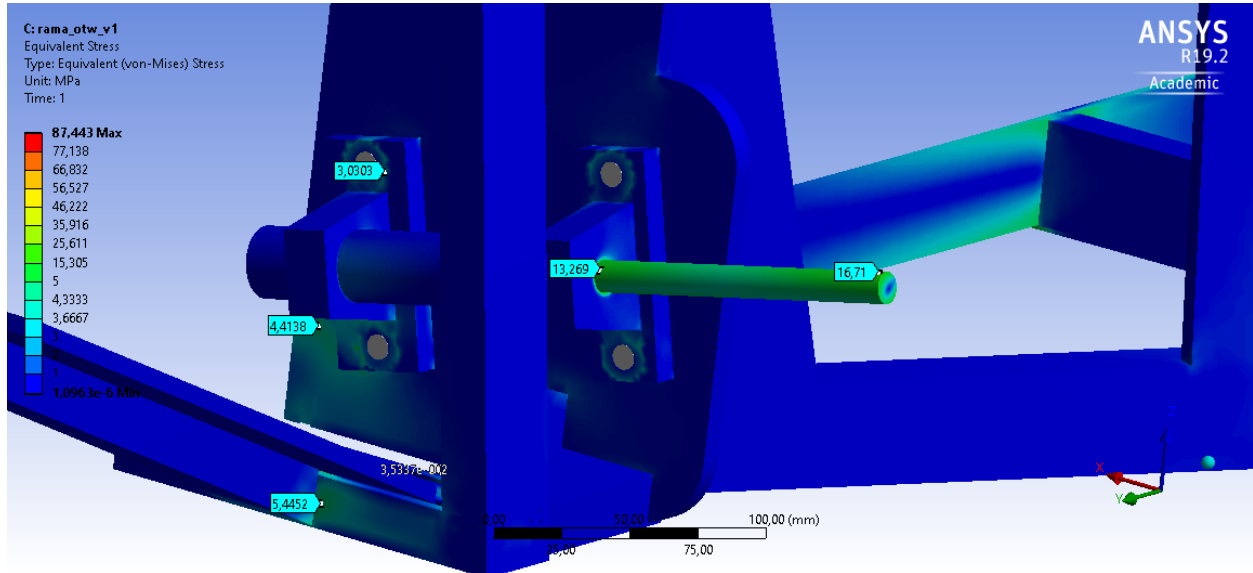


Figure 9: *Reduced stress values in the area of the rear shaft*
(source: own data)

As a result of the FEM analysis, the total displacements of the structure and the stress distribution in the frame were obtained. The total displacement in the frame was 1.65 mm and occurred at the top of the frame of the left battery (Fig. 10).

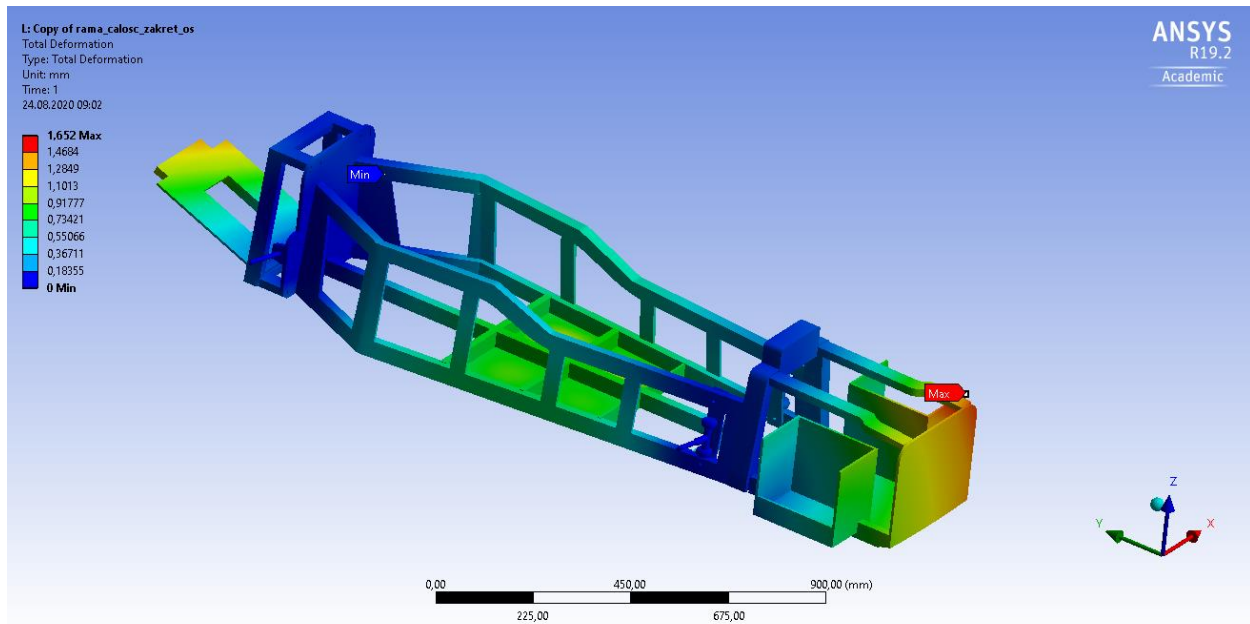


Figure 10: Total displacements in the car frame
(source: own data)

The displacement in the vicinity of the driver's seat ranged from 0.8-1.13 mm. The displacement near the plate under the motor was 0.6-1.24 mm.

The maximum reduced stresses (von Mises) amounted to 94 MPa and took place at the support point, the left front shaft. The average stresses occurring in the entire frame amounted to approximately 0.5 MPa. The stresses in the frame attachment of the area of the bodywork attachment to the frame amounted to 0.2 MPa in the area of the front attachment and approximately 0.4 MsPa in the vicinity of the rear attachment of the bodywork.

6. Conclusions

- The conducted study was subject to limitations from the size of the computational model. The geometry of the analyzed frame model had to be significantly simplified in order to reduce computation time. The far-reaching simplifications and the potentially large size of the mesh created in some areas may have affected the calculation results.
- Due to its hardness, oak wood is characterized by a significantly lower displacement (2.5 times less compared to pine wood and three times less than plywood) as a result of the load than other tested materials.

- For a glued joint, the stresses obtained are very similar for each material (difference below 1%), so they result from the characteristics of the joint and the material of the joint, not the type of wood that has been joined.
- For the screw joint, the stresses for oak wood are twice as high as for pinewood and plywood. This is due to the high rigidity of the oak wood.
- The frame design was done correctly, since the car frame is not subjected to stresses exceeding the allowable stresses of the material, both under static load and when driving in a corner as a result of the centrifugal force.
- In future research, the process of preparing a model of such a complex structure for FEA analysis should be improved. Other potential ways of assembling the timber members should also be verified in order to select the optimal solution for the fabrication of the designed frame.

REFERENCES

- Apay, A. C. (2012). Finite element analysis of wooden chair strength in free drop. *International Journal of Physical Sciences*, 7(7), 1105-1114. <https://doi.org/10.5897/IJPS11.1229>
- Baier, A., Grabowski, Ł., Stebel, Ł., Komander, M., Konopka, P., Kołodziej, A., & Żur, P. (2018). Numeric analysis of airflow around the body of the Silesian Greenpower vehicle. In *MATEC Web of Conferences* (Vol. 178, p. 05014). EDP Sciences.
- Bąk, R., & Burczyński, T. (2001). *Wytrzymałość materiałów z elementami ujęcia komputerowego*. Wydawnictwa Naukowo-Techniczne.
- Groom, L. H., Mott, L., & Shaler, S. (2002). Mechanical properties of individual southern pine fibres. Part I. Determination of variability of stress-strain curves with respect to tree height and juvenility. *Wood and Fiber Science* 34 (1): 14-27.
- Hunt, J. F. (2004). 3D engineered fiberboard: Finite element analysis of a new building product. In 2004 International ANSYS Conference, Pittsburg, PA, May 24-26, 2004
- Jasieńko, J., Nowak, T., & Karolak, A. (2014). Historyczne złącza ciesielskie. *Wiadomości konserwatorskie*. <http://www.timberbits.com/blog/history-of-woodworking/> [retrieved 28.04.2020]

Karaöali, Ö., & Ulguel, A. T. (2014). Finite Element Analysis of Pallet-Nail Materials Used in Pallet Joint Design for Material Handling Works. *Acta Physica Polonica, A.*, 125(2).

<https://doi.org/10.12693/APhysPolA.125.183>

Štědroňová, A. (2010). Problematika biokoroze ve stavebnictví.

Tankut, N., Tankut, A. N., & Zor, M. (2014). Finite element analysis of wood materials. *Drvna industrija: Znanstveni časopis za pitanja drvne tehnologije*, 65(2), 159-171.

<https://doi.org/10.5552/drind.2014.1254>

Zachariah, A. T. (2006). Finite Element Modelling of Adhesive Interface between Steel and CFRP (Master's thesis). <https://doi.org/10.1051/matecconf/201817805014>

Žur, P., Baier, A., & Kołodziej, A. (2020). Chassis Geometry Optimization based on 3D-scans of the Ergonomic Driving Position. *International Journal of Mechanical Engineering and Robotics Research*, 9(8).

<https://doi.org/10.18178/ijmerr.9.8.1213-1218>